Cent. Eur. J. Phys. • 6(4) • 2008 • 808-811
DOI: 10.2478/s11534-008-0115-0

VERSITA

Central European Journal of **Physics**

Electronic properties of austenite and martensite Fe-9%Mn alloys

Research Article

Ercan Uçgun*, Hamza Y. Ocak

Dumlupınar University, Faculty of Arts and Sciences, Department of Physics Kütahya, Turkey

Received 15 February 2008; accepted 21 July 2008

Abstract: We calculate the electronic properties of austenite and martensite Fe–9%Mn alloys using the self consistent full-potential linearized-plane-wave method under the generalized gradient approximation full lattice relaxation. By minimizing total-energy, the lattice constants in their ground states were determined. We discuss the total energy dependence of the volume, and density of states (DOS).

PACS (2008): 61.66.Dk, 62.20.D-, 71.15.Mb, 71.20.Be

Keywords: WIEN2k • DOS • Fe-Mn Alloys

1. Introduction

Fe-Mn alloys at room temperature are fcc crystal structures but can be changed to bcc, bct and hcp. These alloys are widely used for developing stainless austenite steels especially for use in critical temperature ranges, aggressive environments and other severe external conditions. Bolton *et al.* [1] showed that Fe-Mn alloys containing 4–10%Mn have a Lath martensitic structure on cooling from the austenite phase field, and Schumann [2] examined the dependence of α'-martensite formation on the manganese content of Fe-Mn alloys and reported the formation of α'-martensite when the manganese content is less than 10%. The α'-phase is formed by plastically deformation of the samples at low transformation temperatures. It has been well established that, depending on the manganese content, three distinct types of martensite structures, namely, ϵ (hcp), α' (bcc), and α (bct) martensites, are formed in Fe-Mn binary alloys [3]. Although both phases generally appear together, in some Fe-Mn alloys one type can be formed without formation of the other [4].

Deformation-induced formation of α'-martensite in Fe-Mn alloys can easily be explained using the model described by Olson and Cohen [5], which is based on the assumption that new sites or embryos for such formation are created by the applied plastic deformation.

Plastic deformation influences the structure and electronic properties of Fe-Mn alloys. These properties of Fe-Mn alloys have been studied theoretically by various research groups [6-11]. The role of theoretical calculations in the area of solid state research has expanded rapidly during the last few years. Such methods are used in calculating the electronic structure and physical properties of solids, and are increasingly used for solving not only fundamental, but also applied problems.

There exists a large amount of experimental information

*E-mail: eucgun@dumlupinar.edu.tr

on the electronic structure and magnetic properties of Fe-Mn alloy because transition metal is a constituent of many important magnetic materials. As a pure element, bcc iron is ferromagnetic with a magnetic moment of 2.2 μ_B. Pure manganese has a very complicated crystal (with a unit cell of 58 atoms) and magnetic structures. Iron-rich Fe_x-Mn_{1-x} bcc alloys ($x > 0.8$) show ferromagnetic order with nonlinear behavior of magnetization that abruptly disappears at $x = 0.8$ [12]. When manganese is alloyed with large amounts of Fe, it forms a bcc lattice and is ferromagnetic. Nuclear magnetic resonance measurements have found a magnetic moment for manganese of order 1.5 to 3.0 μ_B [13]. Iron and manganese couple paramagnetically when the manganese metal is in antiferromagnetic state.

The bcc structure is the most common among the transition metals, and the combination of the axial symmetry and the two atoms per unit cell results in an electronic structure which is more complex in noncubic structures. This complexity is reflected in the Fermi surfaces. The band structures of γ-Mn and γ-Fe were studied by Asano and Yamashita, using Green's function techniques with the Slater exchange approximation [14].

There have been a large number of experimental and theoretical studies for understanding and predicting the electronic structure and the related structural, electrical, and magnetic properties of the 3*d* intermetallic compounds. As 3*d* transition metal elements with strong ferromagnetism, iron and manganese have particularly-filled *d* bands which are localized in energy and space compared to the neighboring well-dispersed *sp* bands. Strong spin exchange splitting between the majority- and minority-spin *d* states cause ferromagnetism at room temperature.

In the last decades several theoretical schemes have been employed to study the magnetic behavior of metallic systems. In this matter the iron based alloys especially have been the focus of attention of the research.

In this work, the electronic structures of fcc and bcc Fe-9%Mn alloys were studied using the WIEN2k program package [15]. Studies on the deformed samples which were numbered II, III and IV are carried out and will be reported soon.

2. Preparing samples

The Fe-9%Mn alloy was prepared by induction melting in an argon atmosphere from pure (99.9%) alloy elements. Samples were homogenized at 1100 °C for sixteen hours and quenched in ice water to initiate martensite formation in the fcc austenite structure. The specimens were examined in a Jeol-200CX Transmission Electron Microscope (TEM) operating at 200kV. TEM observations showed the presence of only α'-type martensite structures. In the austenitic samples which were quenched at room temperature after homogenization. Lattice constants of samples were calculated using diffraction patterns as shown in Table 1 [16].

Table 1. Calculated lattice constants of samples using diffraction patterns.

Sample	Applied physical deformation	a_{fcc} [Å]	a_{bcc} [Å]
I	at nitrogen temperature	3.758	2.882
II	5% at nitrogen temperature	3.719	2.853
III	8.5% at nitrogen temperature	3.737	2.847
IV	27% at nitrogen temperature	3.738	2.852

3. Calculation details

All the calculations reported in this paper are performed by using the self-consistent full-potential linearized augmented-plane-wave (FLAPW) method [15] under the generalized gradient approximation (GGA) in a scalar relativistic version without spin-orbit coupling. We have adopted the Perdew *et al.* exchange-correlation functionals [17] in the GGA calculations. To separate core and valance states, the energy threshold of -6.0 Ry is used. The muffin tin radii (atomic sphere size R_{MT}) were 1.70 au for iron and 1.70 au for manganese in the austenite phase and 1.58 au for iron and 1.58 au for manganese in the martensite phase. To achieve convergence the energy criterion was chosen at 0.00001 Ry. For the number of plane waves, we took $R_{MT}(\max) \times K_{\max} = 7$. One thousand k-points were used in the mesh for the integration procedure, which were leading to 47 inequivalent k-points in the irreducible Brillouin zone. Both the muffin tin radius and the number of k-points were varied to ensure convergence. We used the experimental lattice constants a=7.444475 au (austenite) and a=5.250350 au (martensite).

The supercell approach has been used to study Fe-9%Mn alloys for both martensite and austenite phases containing about nine per cent manganese. The symmetry of the martensite structure is $Im-3m$ and the symmetry of the austenite structure is $Fm-3m$. Therefore, bcc Fe-9%Mn (martensite) and fcc Fe-9%Mn (austenite) structures have been studied and reported here.

For the cubic structures (fcc and bcc) the total energy is calculated as a function of cell volume V. We performed calculations for eleven different volumes in order to optimize V. The calculated total energy as a function of volume was fitted to the Murnaghan equation of state

[18]. From this process the equilibrium volume (V_0), the bulk modulus (B) and the two shear moduli (G' and G) were obtained. Figure 1 shows the fits to the calculated total energy as a function of volume for our alloys. From these graphs the equilibrium volumes of each structure are obtained and the lattice constants calculated using the minimum energy value at the equilibrium volume.

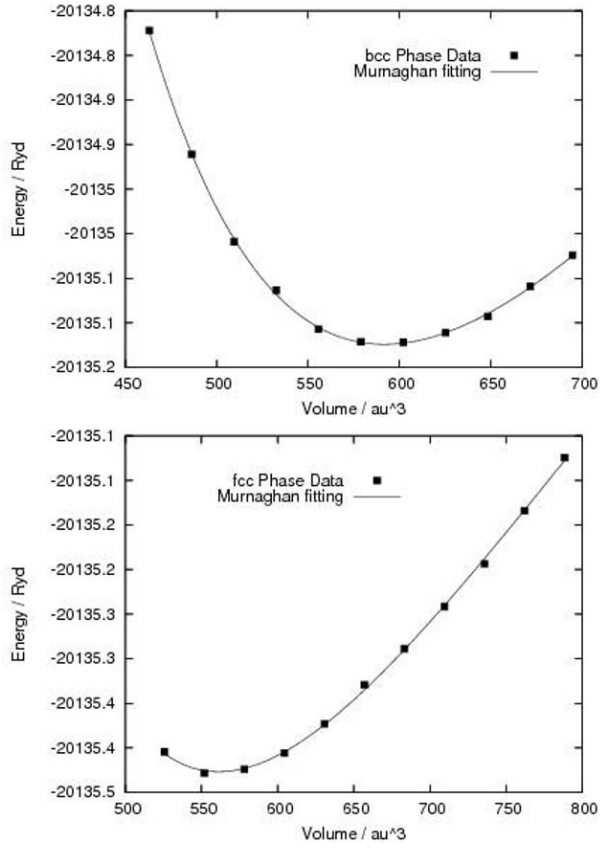

Figure 1. Total energies as a function of volume for martensite phase (upper graph) and austenite phase (below graph).

Table 2. Calculated equilibrium volumes, bulk moduli and energy difference for the austenite and martensite phases for the Sample I.

	$V_0[au^3]$	B [GPa]	G' [GPa]	G [GPa]	ΔE [Ry]
fcc phase	562.4069	86.188	239.306	100.434	0.2131
bcc phase	592.8229	251.389	255.108	25.309	0.2131

In Table 2, we summarize the calculated equilibrium volumes, bulk modulus, the two shear moduli for the austenite and martensite phases, and the energy difference between the minimum energy of these two phases $\Delta E = E_0^{fcc} - E_0^{bcc}$. The stabilities of Fe-9%Mn alloy have been analyzed using the elastic constants. A cubic crystal has three independent elastic moduli: these can be taken to the bulk modulus (B) and two shear moduli, $G' = (C_{11} - C_{12})/2$ and $G = C_{44}$. In this way, the conditions for elastic stability of a cubic lattice are [19]

$$\begin{aligned} B &= (C_{11} + 2C_{12})/3 > 0 \\ G' &= (C_{11} - C_{12})/2 > 0 \\ G &= C_{44} > 0. \end{aligned} \quad (1)$$

We can see that the elastic stability criteria for a cubic crystal are fully filled by the calculated elastic constants for samples. Therefore the samples are locally stable for fcc and bcc structures, as seen in Figure 1. Stability of Fe-9%Mn alloys, to our best knowledge, has not been observed yet in the context of austenite-martensite phase transitions.

Table 3. Calculated and experimental values of lattice parameters for austenite and martensite phases in Sample I.

	a_{fcc} [au]	a_{bcc} [au]
calculated	6.551492	5.292022
experimental	7.444475	5.250350

The calculated lattice parameters for the samples are presented in Table 3 and these parameters for both fcc and bcc alloys are very close to experimental values (3.758 Å and 2.882 Å, respectively) obtained using TEM methods [16]. For the fcc phase we obtained an equilibrium lattice parameter of 6.551492 au; for the bcc phase, 5.292022 au. In Figure 2, we present the calculated electronic densities of states (DOS) for fcc and bcc phases. The solid line corresponds to the fcc phase and the dotted line to the bcc phase; the zero of the energy axis is at the Fermi level (E_F). The bandwidth of bcc phase is slightly larger than that of the fcc phase. Peaks of the bcc phase were better formed.

4. Conclusion

The total energy dependence of the volume and density of states (DOS) was presented for austenite and martensite Fe-9%Mn alloys using the self consistent full-potential linearized-plane-wave (FLAPW) method under the generalized-gradient approximation full lattice relaxation. We observed the stability of Fe-9%Mn alloys in

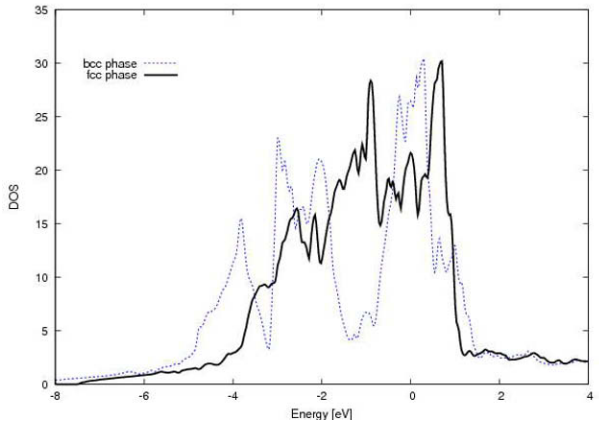

Figure 2. Density of States (DOS) for fcc (solid lines) and bcc (dotted lines) phases.

terms of austenite-martensite phase transitions, analyzing them using elastic constants. The elastic stability criteria were achieved from several samples and we thence concluded that the samples are locally stable for fcc and bcc structures. The calculated lattice parameters for both fcc and bcc alloys were very close to our experimental values obtained from TEM methods.

5. Acknowledgements

This work was supported by the Dumlupınar University within research Project No. 43.

References

[1] J.D. Bolton, E.R. Petty, G.B. Allen, J. Iron Steel Inst. 207, 1314 (1969)
[2] H. Schumann, Arch. Eisenhuttenwes. 40, 1027 (1969)
[3] J.H. Yang, H. Chen, C.M. Wayman, Metall. Trans. 23 A, 1439 (1992)
[4] I. Akgün, T.N. Durlu, Scripta Metall. 31, 1361 (1994)
[5] G.B. Olson, M. Cohen, Metall. Trans. 6 A, 791 (1975)
[6] M.E. Elzain, A.A. Yousif, Phys. Status Solidi B 178, 451 (1993)
[7] Y. Zhou, D. Wang, Y. Kawazoe, Phys. Rev. B 59, 8387 (1999)
[8] D. Spisak, J. Hafner, Phys. Rev. B 61, 11569 (2000)
[9] K. Nakamura, T. Ito, A.J. Freeman, L. Zhong, J.F. Castro, Phys. Rev. B 67, 14405 (2003)
[10] N.I. Kulikov, C. Demangeat, Phys. Rev. B 55, 3533 (1997)
[11] C. Paduini, J.C. Krause, Phys. Rev. B 58, 175 (1998)
[12] J. Hesse, Hyperfine Interactions 47, 357 (1989)
[13] V. Jaccarino, L.R. Walker, G.K. Wertheim, Phys. Rev. Lett. 14, 89 (1965)
[14] S. Asano, J. Yamashita, J. Phys. Soc. Jpn. 31, 1000 (1971)
[15] P. Blaha, K. Schwarz, G.K.H. Madsen, D. Kvasnich, J. Luitz, WIEN2k, An Augmented Plane Wave + Local Orbitals Program for Calculating Crystal Properties (Tech. Uni. Wien, 2001)
[16] E. Çalık, H.Y. Ocak, Journal of the Institute of Science and Technology of Dumlupınar University 4, 105 (2003) (in Turkish)
[17] J.P. Perdew, K. Burke, M. Ernzerhof, Phys. Rev. Lett. 77, 3865 (1996)
[18] D.F. Murnaghan, P. Natl. Acad. Sci. USA 30, 244 (1944)
[19] D.C. Wallace, Thermodynamics of Crystals (Dover Publications Inc., 1998)